Effects of substrates on the nonlinear optical responses of two-dimensional materials

Jianhua Zeng,[1] Jinxiang Li,[1] Hui Li,[1] Qiaofeng Dai,[1] Shaolong Tie,[2] and Sheng Lan[1,*]

[1]*Guangdong Provincial Key Laboratory of Nanophotonic Functional Materials and Devices, School of Information and Optoelectronic Science and Engineering, South China Normal University, Guangzhou 510006, China*
[2]*School of Chemistry and Environment, South China Normal University, Guangzhou 10006, China*
[*]*slan@scnu.edu.cn*

Abstract: We investigated numerically and experimentally the achievement of strongly localized electric field and significantly enhanced second harmonic generation (SHG) in two-dimensional (2D) materials by using dielectric-metal hybrid substrates. Based on the theory of thin film interference, it was revealed that the strongest localization of electric field in a 2D material, which corresponds to the largest absorption in the metal film, could be achieved by minimizing the reflection of the combined structure (i.e., 2D material + hybrid substrate) because the transmission through the combined structure was negligible. By using MoS_2 as an example, it was demonstrated that a SHG enhancement factor of ~6 could be achieved in the 17-nm-thick MoS_2 layer on an Au/SiO_2 substrate as compared with the single-layer MoS_2 on the commonly used SiO_2/Si substrates with highly efficient SHG. By employing a SiO_2-$SnO_2/Ag/SiO_2$ substrate in which a 20-nm-thick dielectric film of SiO_2-SnO_2 was inserted in between the MoS_2 layer and the Ag film, a SHG enhancement factor as large as ~18 could be realized in the 9-nm-thick MoS_2 layer. Numerical simulations based on the finite-difference time-domain technique were employed to derive the enhancement factors for SHG and it was revealed that for thick MoS_2 layers the SHG intensity is dominated mainly by the localization of electric field induced by the dielectric-metal hybrid substrates. The dependence of the SHG enhancement factor on the thickness of the MoS_2 layer was found to be modified when the dielectric-metal hybrid substrates were adopted.

OCIS codes: (240.0310) Thin films; (310.4165) Multilayer design; (190.2620) Harmonic generation and mixing; (190.4400) Nonlinear optics, materials.

References and links

1. L. Liu, S. B. Kumar, Y. Ouyang, and J. Guo, "Performance limits of monolayer transition metal dichalcogenide transistors," IEEE Trans. Electron. Dev. **58**(9), 3042–3047 (2011).
2. Y. Yoon, K. Ganapathi, and S. Salahuddin, "How good can monolayer MoS_2 transistors be?" Nano Lett. **11**(9), 3768–3773 (2011).
3. H. Wang, L. Yu, Y. H. Lee, Y. Shi, A. Hsu, M. L. Chin, L. J. Li, M. Dubey, J. Kong, and T. Palacios, "Integrated circuits based on bilayer MoS_2 transistors," Nano Lett. **12**(9), 4674–4680 (2012).
4. B. Radisavljevic, M. B. Whitwick, and A. Kis, "Integrated circuits and logic operations based on single-layer MoS_2," ACS Nano **5**(12), 9934–9938 (2011).
5. S. Bertolazzi, J. Brivio, and A. Kis, "Stretching and breaking of ultrathin MoS_2," ACS Nano **5**(12), 9703–9709 (2011).
6. Q. He, Z. Zeng, Z. Yin, H. Li, S. Wu, X. Huang, and H. Zhang, "Fabrication of flexible MoS_2 thin-film transistor arrays for practical gas-sensing applications," Small **8**(19), 2994–2999 (2012).
7. J. Pu, Y. Yomogida, K. K. Liu, L. J. Li, Y. Iwasa, and T. Takenobu, "Highly flexible MoS_2 thin-film transistors with ion gel dielectrics," Nano Lett. **12**(8), 4013–4017 (2012).
8. Z. Yin, H. Li, H. Li, L. Jiang, Y. Shi, Y. Sun, G. Lu, Q. Zhang, X. Chen, and H. Zhang, "Single-layer MoS_2 phototransistors," ACS Nano **6**(1), 74–80 (2012).
9. H. S. Lee, S. W. Min, Y. G. Chang, M. K. Park, T. Nam, H. Kim, J. H. Kim, S. Ryu, and S. Im, "MoS_2 nanosheet phototransistors with thickness-modulated optical energy gap," Nano Lett. **12**(7), 3695–3700 (2012).

#252118 Received 16 Oct 2015; revised 21 Nov 2015; accepted 24 Nov 2015; published 1 Dec 2015

10. M. Shanmugam, T. Bansal, C. A. Durcan, and B. Yu, "Molybdenum disulphide/titanium dioxide nanocomposite-poly 3-hexylthiophene bulk heterojunction solar cell," Appl. Phys. Lett. **100**(15), 153901 (2012).
11. K. S. Novoselov, A. K. Geim, S. V. Morozov, D. Jiang, Y. Zhang, S. V. Dubonos, I. V. Grigorieva, and A. A. Firsov, "Electric field effect in atomically thin carbon films," Science **306**(5696), 666–669 (2004).
12. K. S. Novoselov, D. Jiang, F. Schedin, T. J. Booth, V. V. Khotkevich, S. V. Morozov, and A. K. Geim, "Two-dimensional atomic crystals," Proc. Natl. Acad. Sci. U.S.A. **102**(30), 10451–10453 (2005).
13. K. F. Mak, C. Lee, J. Hone, J. Shan, and T. F. Heinz, "Atomically thin MoS_2: A new direct-gap semiconductor," Phys. Rev. Lett. **105**(13), 136805 (2010).
14. A. Splendiani, L. Sun, Y. Zhang, T. Li, J. Kim, C. Y. Chim, G. Galli, and F. Wang, "Emerging photoluminescence in monolayer MoS_2," Nano Lett. **10**(4), 1271–1275 (2010).
15. K. F. Mak, K. He, J. Shan, and T. F. Heinz, "Control of valley polarization in monolayer MoS_2 by optical helicity," Nat. Nanotechnol. **7**(8), 494–498 (2012).
16. H. Zeng, J. Dai, W. Yao, D. Xiao, and X. Cui, "Valley polarization in MoS_2 monolayers by optical pumping," Nat. Nanotechnol. **7**(8), 490–493 (2012).
17. T. Cao, G. Wang, W. Han, H. Ye, C. Zhu, J. Shi, Q. Niu, P. Tan, E. Wang, B. Liu, and J. Feng, "Valley-selective circular dichroism of monolayer molybdenum disulphide," Nat. Commun. **3**(2), 887 (2012).
18. S. Tongay, J. Zhou, C. Ataca, K. Lo, T. S. Matthews, J. Li, J. C. Grossman, and J. Wu, "Thermally driven crossover from indirect toward direct bandgap in 2D semiconductors: $MoSe_2$ versus MoS_2," Nano Lett. **12**(11), 5576–5580 (2012).
19. R. Ganatra and Q. Zhang, "Few-layer MoS_2: a promising layered semiconductor," ACS Nano **8**(5), 4074–4099 (2014).
20. H. Zhu, Y. Wang, J. Xiao, M. Liu, S. Xiong, Z. J. Wong, Z. Ye, Y. Ye, X. Yin, and X. Zhang, "Observation of piezoelectricity in free-standing monolayer MoS_2," Nat. Nanotechnol. **10**(2), 151–155 (2014).
21. Y. Lin, X. Ling, L. Yu, S. Huang, A. L. Hsu, Y.-H. Lee, J. Kong, M. S. Dresselhaus, and T. Palacios, "Dielectric screening of excitons and trions in single-layer MoS_2," Nano Lett. **14**(10), 5569–5576 (2014).
22. R. W. Boyd, *Nonlinear Optics*, 3rd ed. (Academic, 2008).
23. N. Kumar, S. Najmaei, Q. Cui, F. Ceballos, P. M. Ajayan, J. Lou, and H. Zhao, "Second harmonic microscopy of monolayer MoS_2," Phys. Rev. B **87**(16), 161403 (2013).
24. L. M. Malard, T. V. Alencar, A. P. M. Barboza, K. F. Mak, and A. M. de Paula, "Observation of intense second harmonic generation from MoS_2 atomic crystals," Phys. Rev. B **87**(20), 201401 (2013).
25. Y. Li, Y. Rao, K. F. Mak, Y. You, S. Wang, C. R. Dean, and T. F. Heinz, "Probing symmetry properties of few-layer MoS_2 and h-BN by optical second-harmonic generation," Nano Lett. **13**(7), 3329–3333 (2013).
26. D. J. Clark, C. T. Le, V. Senthilkumar, F. Ullah, H.-Y. Cho, Y. Sim, M.-J. Seong, K.-H. Chung, Y. S. Kim, and J. I. Jang, "Near bandgap second-order nonlinear optical characteristics of MoS_2 monolayer transferred on transparent substrates," Appl. Phys. Lett. **107**(13), 131113 (2015).
27. H. Zeng, G.-B. Liu, J. Dai, Y. Yan, B. Zhu, R. He, L. Xie, S. Xu, X. Chen, W. Yao, and X. Cui, "Optical signature of symmetry variations and spin-valley coupling in atomically thin tungsten dichalcogenides," Sci. Rep. **3**(7444), 1608 (2013).
28. M. Grüning and C. Attaccalite, "Second harmonic generation in *h*-BN and MoS_2 monolayers: role of electron-hole interaction," Phys. Rev. B **89**(8), 081102 (2014).
29. M. M. Ugeda, A. J. Bradley, S.-F. Shi, F. H. da Jornada, Y. Zhang, D. Y. Qiu, W. Ruan, S. K. Mo, Z. Hussain, Z. X. Shen, F. Wang, S. G. Louie, and M. F. Crommie, "Giant bandgap renormalization and excitonic effects in a monolayer transition metal dichalcogenide semiconductor," Nat. Mater. **13**(12), 1091–1095 (2014).
30. G. Gao, W. Gao, E. Cannuccia, J. Taha-Tijerina, L. Balicas, A. Mathkar, T. N. Narayanan, Z. Liu, B. K. Gupta, J. Peng, Y. Yin, A. Rubio, and P. M. Ajayan, "Artificially stacked atomic layers: toward new van der Waals solids," Nano Lett. **12**(7), 3518–3525 (2012).
31. J. Bardeen, "Electron correlation and screening effects in related to surface physics," Surf. Sci. **2**(6), 381–388 (1964).
32. K. S. Yee, "Numerical solution of boundary value problems involving Maxwell's equations in isotropic media," IEEE Trans. Antenn. Propag. **14**(3), 302–307 (1966).
33. C. C. Shen, Y. T. Hsu, L. J. Li, and H. L. Liu, "Charge dynamics and electronic structures of monolayer MoS_2 films grown by chemical vapor deposition," Appl. Phys. Express **6**(12), 125801 (2013).
34. R. A. Neville and B. L. Evans, "The band edge excitons in 2H-MoS_2," Phys. Status Solidi **73**(2), 597–606 (1976).
35. C. Hubert, L. Billot, P. M. Adam, R. Bachelot, P. Royer, J. Grand, D. Gindre, K. D. Dorkenoo, and A. Ford, "Role of surface plasmon in second harmonic generation from gold nanorods," Appl. Phys. Lett. **90**(18), 181105 (2007).
36. M. A. Kats, R. Blanchard, P. Genevet, and F. Capasso, "Nanometre optical coatings based on strong interference effects in highly absorbing media," Nat. Mater. **12**(1), 20–24 (2012).
37. M. A. Kats, S. J. Byrnes, R. Blanchard, M. Kolle, P. Genevet, J. Aizenberg, and F. Capasso, "Enhancement of absorption and color contrast in ultra-thin highly absorbing optical coatings," Appl. Phys. Lett. **103**(10), 101104 (2013).
38. M. A. Kats, R. Blanchard, S. Ramanathan, and F. Capasso, "Thin-film interference in lossy, ultra-thin layers," Opt. Photonics News **25**(1), 40–47 (2014).
39. J. Zeng, M. Yuan, W. Yuan, Q. Dai, H. Fan, S. Lan, and S. Tie, "Enhanced second harmonic generation of MoS_2 layers on a thin gold film," Nanoscale **7**(32), 13547–13553 (2015).

#252118 Received 16 Oct 2015; revised 21 Nov 2015; accepted 24 Nov 2015; published 1 Dec 2015

40. H. Li, Q. Zhang, C. C. R. Yap, B. K. Tay, T. H. T. Edwin, A. Olivier, and D. Baillargeat, "From bulk to monolayer MoS_2: evolution of raman scattering," Adv. Funct. Mater. **22**(7), 1385–1390 (2012).

1. Introduction

In recent years, two-dimensional (2D) materials have attracted great interest owing to their potential applications in logic electronics [1,2], integrated circuits [3,4], flexible electronics [5–7], optoelectronics and nanophotonics [8–12]. Apart from graphene, MoS_2 is the most intensively and extensively studied 2D material [13–21]. So far, the physical properties of MoS_2, especially the mechanical, electronic and optical properties, have been deeply investigated. Recently, the nonlinear optical responses of MoS_2 have become the focus of many studies because they play an important role in the photonic applications in which ultrafast laser pulses with high peak powers are generally used. Although bulk MoS_2 crystal with 2H stacking order is expected to have vanished second-order nonlinear susceptibility ($\chi^{(2)}$) because of the inversion symmetry [22], it has been demonstrated that MoS_2 with odd layers, especially the single-layer one [23–26], exhibit efficient second harmonic generation (SHG) arising from the breaking of the inversion symmetry. As a result, an oscillation of the SHG intensity with increasing layer number has been oobserved [25,27].

Very recently, several research groups reported independently the observation of highly efficient SHG from single-layer MoS_2 and the dependence of the SHG intensity on the layer number of MoS_2 and the polarization of the excitation laser [23–26]. Kumar et al. derived a second-order nonlinear susceptibility $\chi^{(2)}$ on the order of $\sim 10^{-7}$ m/V for single-layer MoS_2 and found a reduction of SHG by a factor of seven in trilayer MoS_2 and by two orders of magnitudes in MoS_2 with even layers [23]. Large second-order nonlinear susceptibility with a similar value was also observed by Malard et al [24]. Li et al. measured and compared the SHG in thin MoS_2 and h-BN with one to five layers and also observed strong SHG from materials with odd layers and no appreciable SHG from materials with even layers [25]. Clark et al. investigated the second-order nonlinear optical properties of CVD-grown single-layer MoS_2 transferred onto transparent substrates such as fused silica and polyethylene terephthalate [26]. For single-layer MoS_2, an enhancement in SHG originating from the enhanced electron hole interaction was also analyzed theoretically and demonstrated experimentally [28–30]. The enhanced interaction between electrons and holes arises from the reduced screening effect, leading to a binding energy of excitons much larger than that in bulk MoS_2 [29].

So far, the substrates commonly used for studying MoS_2 are SiO_2 and SiO_2/Si substrates because atomically thin MoS_2 layers on these substrates exhibit different colors which depend strongly on the thicknesses of the MoS_2 layers. Since the color of a thin MoS_2 layer is governed by the reflection spectrum of the combined structure (i.e., MoS_2 + substrate), the substrate has great influence on the color of the MoS_2 layer placed on it. This feature makes it easy to identify MoS_2 with few layers. For SiO_2 or SiO_2/Si substrates, it seems that the inversion symmetry plays a key role in determining the SHG intensity of the MoS_2 layer because of the low refractive index of SiO_2, especially for MoS_2 with few layers. A simple analysis or simulation reveals that strong localization of electric field cannot be achieved in the MoS_2 layers on a SiO_2/Si substrate because of the low refractive index of SiO_2. However, this feature will be changed when a dielectric-metal hybrid substrate with a thin metal film is adopted. Strong localization of electric field may be achieved by using the dielectric-metal hybrid substrate which will modify significantly both the linear and nonlinear optical responses of the MoS_2 layer. Apparently, the use of dielectric-metal hybrid substrates with a thin metal film will lead to the breaking of inversion symmetry. In addition, dielectric-metal hybrid substrates also induce a variation of screening effect through correlation effects [28–31]. All these effects will facilitate the SHG in MoS_2 layers on dielectric-metal hybrid substrates.

In this article, the effects of dielectric-metal hybrid substrates on the enhancement of the nonlinear optical responses of the MoS_2 layers were investigated both numerically and experimentally. Based on the theory of thin film interference, it was revealed that strong

#252118 Received 16 Oct 2015; revised 21 Nov 2015; accepted 24 Nov 2015; published 1 Dec 2015

localization of electric field in the MoS_2 layer could be achieved and the dependence of the SHG enhancement factor on the thickness of the MoS_2 layer would be modified by using dielectric-metallic hybrid substrates such as Au/SiO_2 and SiO_2-$SnO_2/Ag/SiO_2$ substrates. Different from the MoS_2 layers on the commonly used SiO_2/Si substrates where the strongest SHG intensity was observed in single-layer MoS_2, the strongest SHG intensity was achieved in a 17-nm-thick (~26 atomic layers) MoS_2 layer on the Au/SiO_2 substrate with an enhancement factor of ~6 and in a 9-nm-thick (~14 atomic layers) MoS_2 layer on the SiO_2-$SnO_2/Ag/SiO_2$ substrate with an enhancement factor of ~18. Numerical simulations based on the finite-difference time-domain (FDTD) technique were employed to derive the SHG enhancement factors and it was revealed that for thick MoS_2 layers the SHG intensity was dominated mainly by the localization of the electric field induced by the dielectric-metallic hybrid substrates.

2. Experimental details and numerical methods

MoS_2 layers with different thicknesses were exfoliated on a SiO_2/Si substrate with a 300-nm-thick SiO_2 film, an Au/SiO_2 substrate with a 50-nm-thick Au film, and a SiO_2-$SnO_2/Ag/SiO_2$ substrate composed of a 20-nm-thick SiO_2-SnO_2 layer and a 50-nm-thick Ag film. The refractive index of the SiO_2-SnO_2 layer, which was used to protect the Ag film from being oxidized, is ~1.7. The colors exhibited by the MoS_2 layers were examined under a microscope. The Raman spectra of the MoS_2 was measured by using a Raman spectrometer (Invia, Renishaw) at an excitation wavelength of 514 nm. A 800-nm femtosecond (fs) laser light with a repetition rate of 76 MHz and a duration of 130 fs delivered by a fs oscillator (Mira 900S, Coherent) was focused on the MoS_2 layers by using the 60 × objective lens (NA = 0.85) of an inverted microscope (Axio Observer A1, Zeiss), the excitation spot was estimated to be ~2 μm in diameter. The nonlinear optical signals generated by the MoS_2 layers were collected by using the same objective lens and directed to a combination of a spectrometer (SR-500i-B1, Andor) and a coupled-charge device (DU970N, Andor) for analysis.

For the calculation of the reflection spectra of the MoS_2 layers and the electric field distributions inside the MoS_2 layers, the FDTD technique was employed [32]. In the numerical simulation, we used a non-uniform grid in which the MoS_2 layer was cut into 10 divisions. Thus, the minimum grid size depended on the thickness of the MoS_2 layer. In addition, a perfectly matched layer boundary condition was employed. The chromaticity coordinates for the MoS_2 layers were derived from the reflection spectra based on the theory of colorimetry. In the numerical simulation, the wavelength dependent complex refractive indexes for single-layer and bulk MoS_2 were chosen to be values that are commonly used [33,34]. In the calculation of the electric field enhancement factors, a continuous wave was employed to approximate the pulse train used in the experiments. The complex refractive indexes for different materials used in the numerical simulation are summarized in Table 1.

Table 1. Complex refractive indexes of MoS_2 (including single-layer and bulk MoS_2), Au, Ag, SiO_2-SnO_2, SiO_2 and Si used in the calculation of the electric field intensity distributions in the MoS_2 layers with different thicknesses on the SiO_2/Si, Au/SiO_2, and SiO_2- $SnO_2/Ag/SiO_2$ substrates

	λ	indexes			λ	indexes	
	(nm)	*n*	*k*		(nm)	*n*	*k*
1L MoS_2	800	4.626	0	SiO_2	800	1.450	0
	400	3.544	4.890		400	1.470	0
bulk MoS_2	800	5.392	0.058	Si	800	3.681	0.005
	400	4.252	3.725		400	5.587	0.303
Au	800	0.154	4.895	Ag	800	0.144	5.289
	400	1.469	1.953		400	0.173	1.95
SiO_2- SnO_2	800	1.700	0				
	400	1.700	0				

#252118 Received 16 Oct 2015; revised 21 Nov 2015; accepted 24 Nov 2015; published 1 Dec 2015

3. Results and discussion

3.1 Principle of electric field localization in two-dimensional materials

Physically, the SHG intensity of the MoS_2 layer can be expressed as follows [35]:

$$I_{SHG} \propto f^4(\lambda) f^2(\lambda/2) I_{in} \quad (1)$$

where I_{SHG} and I_{in} are the intensities of the second harmonic and incident light, $f(\lambda) = |E(\lambda)/E_0|$ and $f(\lambda/2) = |E(\lambda/2)/E_0|$ denote the electric field enhancement factors at the wavelengths of the fundamental light and the second harmonic, respectively. In our experiments, we chose λ = 800 nm at which the imaginary part of the complex refractive index of MoS_2 is negligible. In this case, the second harmonic appeared at 400 nm where the complex refractive index of MoS_2 has a large imaginary part. As a result, $f(\lambda/2)$ cannot be large and the SHG intensity is mainly determined by $f(\lambda)$. Therefore, how to achieve a strong localization of the fundamental light becomes the key point for realizing a large enhancement in SHG.

As schematically shown in Fig. 1(a), the localization of electric field in a 2D material (e.g., MoS_2) placed on a metal (Au)-dielectric (SiO_2) hybrid substrate can be analyzed by using the theory of thin film interference [36–38]. For the fundamental light at ~800 nm, the MoS_2 layer is transparent and the absorption takes place mainly in the Au film. Thus, the stronger the electric field localization, the larger the absorption is. Since the transmission of the fundamental light through the Au film is quite small, the strongest localization of electric field, which corresponds to the largest absorption in the Au film, can be achieved by minimizing the reflection of the combined structure (MoS_2 + substrate). As shown in Fig. 1(a), the fundamental light is incident on the surface of the MoS_2 layer, leading to the first reflected light $\boldsymbol{r}_0$ with a phase shift of π [36–38]. The second reflected light $\boldsymbol{r}_1$ is generated by the Au film and its phase shift contains the phase change induced by the Au film and the phase accumulated by the round trip of the light in the MoS_2 layer. Same is the successive reflected light $\boldsymbol{r}_n$ (n = 2, 3, …). If the thickness of the MoS_2 layer is appropriate, a phase shift of 0 can be obtained for the successive reflected light $\boldsymbol{r}_n$, leading to the destructive interference between the first reflected light $\boldsymbol{r}_0$ and the successive reflected light $\boldsymbol{r}_n$ (n = 1, 2, …) and thus the minimum reflection from the combined structure. In this case, a strong localization of electric field can be established in the MoS_2 layer, leading to a large enhancement in SHG. Although the absorption of the fundamental light takes place mainly in the metal film, it is a detriment for the electric field localization in the MoS_2 layer. Intuitively, the absorption in the thin metal film can be reduced by inserting a dielectric film in between the MoS_2 layer and the metal film, as schematically shown in Fig. 1(b) for a SiO_2-SnO_2/Ag/SiO_2 substrate.

#252118 Received 16 Oct 2015; revised 21 Nov 2015; accepted 24 Nov 2015; published 1 Dec 2015

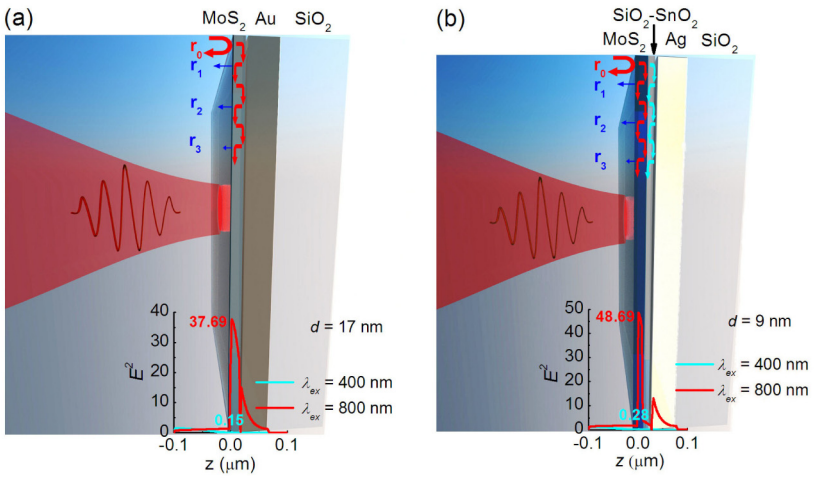

Fig. 1. Schematic showing the localization of electric field in the 17-nm-thick MoS_2 layer on the Au/SiO_2 substrate (a) and in the 9-nm-thick MoS_2 layer on the SiO_2-SnO_2/Ag/SiO_2 substrate (b). The electric field intensity ($|E|^2$) distributions and the corresponding enhancement factors in the two structures calculated at 800 and 400 nm are also presented.

3.2 Dependence of reflection, transmission and absorption spectra and SHG enhancement factor on substrates

Having understood the principle of electric field localization and established the relationship between the reflection and the electric field localization, we can calculate the dependence of the reflection, absorption and transmission of the combined structure on the thickness of the MoS_2 layer in order to find out the appropriate thickness for the MoS_2 layer. The results for the MoS_2 layers on the Au/SiO_2 and SiO_2-SnO_2/Ag/SiO_2 substrates are shown in Figs. 2(a) and 2(b), respectively. In Fig. 2(a), one can see that the thickness at which the maximum absorption is observed coincides with that for the minimum reflection, in good agreement with the analysis presented above. The minimum reflection is observed at a thickness of ~17 nm, implying that the strongest localization of electric field and the largest enhancement in SHG can be achieved in the 17-nm-thick MoS_2 layer. In order to confirm the predicted electric field localization, we calculated the electric field intensity ($|E|^2$) distributions at both 800 and 400 nm for the 17-nm-thick MoS_2 layer on the Au/SiO_2 substrate, as shown in Fig. 1(a). As expected, the enhancement factor for the electric field intensity at 800 nm is 37.69, which is much larger than that at 400 nm (~0.15). This value is also much larger than that for the single-layer MoS_2 on the SiO_2/Si substrate which is ~2.31 (not shown). This result indicates that a significant enhancement in SHG, which is dominated by the electric field enhancement at 800 nm, can be realized by using a dielectric-metal hybrid substrate. In Fig. 2(b), a similar thickness dependence of the reflection, absorption and transmission is observed for the MoS_2 layers on the SiO_2-SnO_2/Ag/SiO_2 substrate. The major difference is the reduction in both the absorption and the transmission due to the introduction of the thin SiO_2-SnO_2 layer. The minimum reflection appears at ~11 nm where the strongest localization of electric field is expected. After considering the electric field enhancement factor at 400 nm, it is found that the largest enhancement factor for SHG is obtained at ~9 nm. Similarly, we calculated the electric field intensity distributions at both 800 and 400 nm for the 9-nm-thick MoS_2 layer on the SiO_2-SnO_2/Ag/SiO_2 substrate, as shown in Fig. 1(b). As expected, the enhancement factor at 800 nm is further increased to 48.69, leading to a further increase in the SHG intensity by a factor of ~3. It implies the significant enhancement in SHG can be realized by properly designing the structure of the dielectric-metal hybrid substrate. In Fig. 2(c), we present the thickness dependence of the SHG enhancement factor calculated for the three types of substrates by using Eq. (1). It can be seen that for the SiO_2/Si substrate the

#252118 Received 16 Oct 2015; revised 21 Nov 2015; accepted 24 Nov 2015; published 1 Dec 2015

strongest SHG is observed in single-layer MoS_2. Owing to the existence of the dielectric-metal hybrid substrate, the strongest SHG is achieved in the 17-nm-thick MoS_2 layer for the Au/SiO_2 substrate and in the 9-nm-thick MoS_2 layer for the SiO_2-SnO_2/Ag/SiO_2 substrate. It is noticed that an increase in the SHG enhancement factor with decreasing thickness is observed for the MoS_2 layers on the SiO_2-SnO_2/Ag/SiO_2 substrate when the thicknesses becomes smaller than ~3 nm.

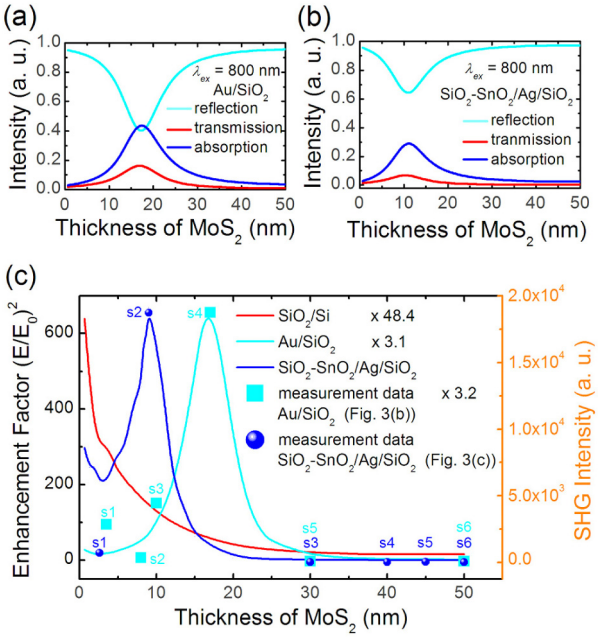

Fig. 2. Thickness dependence of reflection, transmission and absorption spectra calculated for the MoS_2 layer on the Au/SiO_2 (a) and SiO_2-SnO_2/Ag/SiO_2 (b) substrates at the wavelength of 800 nm. A comparison of the thickness dependence of the SHG enhancement factor calculated for the three types of substrates is shown (c). The relative SHG intensities measured for the MoS_2 layers with different thicknesses on the Au/SiO_2 and SiO_2-SnO_2/Ag/SiO_2 substrates are also provided.

3.3 Nonlinear response spectra measured for the MoS_2 layers with different thicknesses on different substrates

The color of a MoS_2 layer depends not only on the thickness of the MoS_2 layer but also on the substrate employed. Some typical colors exhibited by the MoS_2 layers with different thicknesses are shown in Figs. 3(a)-3(c). It can be seen that the colors of the MoS_2 layers on the Au/SiO_2 and SiO_2-SnO_2/Ag/SiO_2 substrates are more abundant than those observed for the MoS_2 layers on the SiO_2/Si substrate. Based on the FDTD simulation, one can easily calculate the reflection spectra of the MoS_2 layers and deduce their chromaticity coordinates [39]. By correlating the calculated chromaticity coordinate with the actually observed color, one can give a rough estimation for the thickness of a MoS_2 layer.

The complex refractive index of MoS_2 used in the numerical simulation is shown in Fig. 4(a). It can be seen that the imaginary part of the complex refractive index is quite large at 400 nm and it is close to zero for wavelengths longer than 700 nm. The reflection spectra calculated for the MoS_2 samples (see s1−s6 in Fig. 3(b)) on the Au/SiO_2 substrate and the MoS_2 samples (see s1−s6 in Fig. 3(c)) on the SiO_2-SnO_2/Ag/SiO_2 substrate are shown in Figs. 4(b) and 4(c). The chromaticity coordinates derived from the reflection spectra are presented in Figs. 4(d) and 4(e), respectively. It can be seen that the color of the 17-nm-thick MoS_2

#252118 Received 16 Oct 2015; revised 21 Nov 2015; accepted 24 Nov 2015; published 1 Dec 2015

layer on the Au/SiO_2 substrate appears to be sky blue while that of the 9-nm-thick MoS_2 layer on the SiO_2-SnO_2/Ag/SiO_2 substrate appears to be deep blue.

Since single-layer MoS_2 on the SiO_2/Si substrate was known to possess a large $\chi^{(2)}$ [23,24], we first examined the nonlinear optical responses of a single-layer MoS_2 whose microscope image is shown in Fig. 3(a). The single-layer MoS_2 was confirmed by the Raman spectrum, as shown in Fig. 5. The frequency difference between the in-plane (E^1_{2g}) and out-of-plane (A_{1g}) vibration modes was estimated to be 18.9 cm^{-1}, in good agreement with the previous reports for single-layer MoS_2 [40]. The nonlinear response spectrum measured for the single-layer MoS_2 is shown in Fig. 3(a) where strong SHG is observed. During the measurement, we rotated the laser polarization and recorded the strongest response spectrum. The same procedure was employed in the following measurements. The nonlinear response spectrum of the bulk MoS_2, whose microscope image is also shown in Fig. 3(a), is also provided for comparison. No appreciable SHG signal was detected for the bulk MoS_2 under the same excitation condition. In Fig. 3(b), we compare the nonlinear response spectra of the MoS_2 layers with different thicknesses on the Au/SiO_2 substrate. It can be seen that the SHG intensity depends strongly on the thickness of the MoS_2 layer and the strongest SHG is achieved in the 17-nm-thick MoS_2 layer. The nonlinear response spectra measured for the MoS_2 layers with different thicknesses on the SiO_2-SnO_2/Ag/SiO_2 substrate are presented in Fig. 3(c). It is found that for most MoS_2 layers the SHG intensities are quite weak and the strongest SHG is achieved in the 9-nm-thick MoS_2 layer. In order to see clearly the effects of substrate structure on the SHG, we compare the nonlinear response spectra obtained under the same excitation condition for the single-layer MoS_2, the 17-nm-thick MoS_2 layer, and the 9-nm-thick MoS_2 layer, as shown in Fig. 3(d). It can be seen that the SHG intensity of the 17-nm-thick MoS_2 layer is about 6 times larger than that of the single-layer MoS_2 while an increase by a factor of ~18 is observed for the 9-nm-thick MoS_2 layer. This phenomenon implies that the SHG intensity of MoS_2 can be significantly enhanced by properly designing the substrate structure.

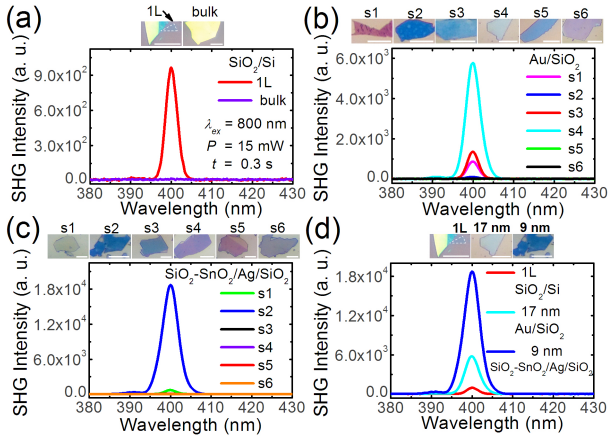

Fig. 3. Nonlinear response spectra measured for the single-layer and bulk MoS_2 on the SiO_2/Si substrate (a), the MoS_2 layers with different thicknesses (s1: ~3.5 nm, s2: ~8 nm, s3: ~10 nm, s4: ~17 nm, s5: ~30 nm, s6: ~50 nm) on the Au/SiO_2 substrate (b), and the MoS_2 layers with different thicknesses (s1: ~2.6 nm, s2: ~9 nm, s3: ~30 nm, s4: ~40 nm, s5: ~45 nm, s6: ~50 nm) on the SiO_2-SnO_2/Ag/SiO_2 substrate (c). A comparison of the nonlinear response spectra for the single-layer MoS_2 on the SiO_2/Si substrate, the 17-nm-thick MoS_2 layer on the Au/SiO_2 substrate and the 9-nm-thick MoS_2 layer on the SiO_2-SnO_2/Ag/SiO_2 substrate is presented in (d). In each case, the microscope images for the MoS_2 layers with different thicknesses are presented on the top of the figure.

#252118 Received 16 Oct 2015; revised 21 Nov 2015; accepted 24 Nov 2015; published 1 Dec 2015

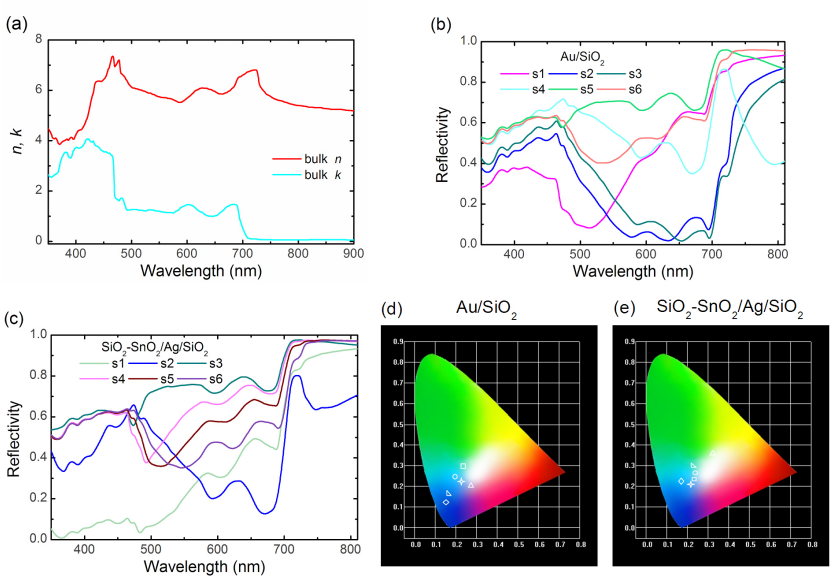

Fig. 4. (a) Complex refractive index of MoS_2 used in the calculation. (b) and (c) show the reflection spectra calculated for the MoS_2 samples (see s1–s6 in Fig. 3(b)) on the Au/SiO_2 substrate and for the MoS_2 samples (see s1–s6 in Fig. 3(c)) on the SiO_2-SnO_2/Ag/SiO_2 substrate. The chromaticity coordinates calculated for the MoS_2 samples (s1–s6) on the Au/SiO_2 and SiO_2-SnO_2/Ag/SiO_2 substrates based on the reflection spectra are shown in (d) and (e) (s1: isosceles triangle; s2: rhombus; s3: right triangle; s4: circle; s5: square; s6: cross star). The calculated chromaticity coordinates are in good agreement with the color shown in Figs. 3(b) and 3(c).

We have measured the Raman spectra for the single-layer MoS_2 layer on the SiO_2/Si substrate, the 17-nm-thick MoS_2 layer on the Au/SiO_2 substrate, and the 9-nm-thick MoS_2 layer on the SiO_2-SnO_2/Ag/SiO_2 substrate, as shown in Fig. 5. For the single-layer MoS_2 layer on the SiO_2/Si substrate, the frequency difference between the in-plane (E^1_{2g}) and out-of-plane (A_{1g}) vibration modes was estimated to be 18.9 cm^{-1}, in good agreement with the previous reports for single-layer MoS_2. The frequency difference between the E^1_{2g} and A_{1g} modes appeared to be larger for the 17-nm-thick MoS_2 layer on the Au/SiO_2 substrate and the 9-nm-thick MoS_2 layer on the SiO_2-SnO_2/Ag/SiO_2 substrate because of the larger thickness. It is also noticed that the intensities of the two Raman modes in the 9-nm-thick MoS_2 layer on the SiO_2-SnO_2/Ag/SiO_2 substrate are stronger than those in the 17-nm-thick MoS_2 layer on the Au/SiO_2 substrate and the single-layer MoS_2 layer on the SiO_2/Si substrate.

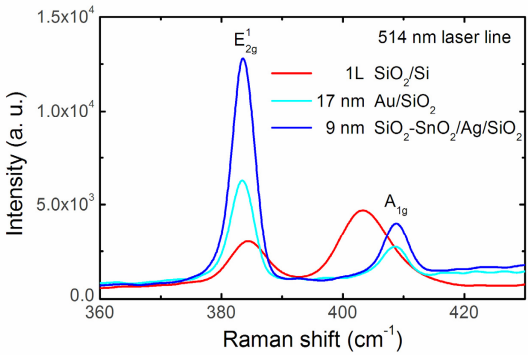

Fig. 5. Raman scattering spectra measured for the single-layer MoS_2 on the SiO_2/Si substrate, the 17-nm-thick MoS_2 layer on the Au/SiO_2 substrate and the 9-nm-thick MoS_2 layer on the SiO_2-SnO_2/Ag/SiO_2 substrate.

#252118 Received 16 Oct 2015; revised 21 Nov 2015; accepted 24 Nov 2015; published 1 Dec 2015

For the single-layer MoS_2 on the SiO_2/Si substrate, the electric field intensity enhancement factors at 800 and 400 nm are 2.31 and 2.48. In this case, the SHG enhancement factor is derived to be 13.2 if the effect of inversion symmetry is not taken into account. For the 17-nm-thick MoS_2 layer on the Au/SiO_2 substrate, the electric field intensity enhancement factor at 800 nm is increased by more than one order of magnitude to 37.69 while that at 400 nm is decreased also by more than one order of magnitude to 0.15. Based on Eq. (1), the SHG enhancement factor is expected to be ~16. However, an enhancement factor of ~6 was observed in the experiments because only the localization of the fundamental light in the MoS_2 layer was considered and the effect of inversion symmetry was not taken into account. As compared with the 17-nm-thick MoS_2 layer, it is found that for the 9-nm-thick MoS_2 layer the electric field intensity enhancement factor at 800 nm is further increased to 48.69 while that at 400 is slightly increased to 0.28, as shown in Fig. 1(b). Consequently, the SHG enhancement factor is further enhanced by a factor of ~3.0, in good agreement with the experimental observations (see Fig. 3(d)).

3.4 Evolution of SHG intensity during the ablation of MoS_2 layers

In order to examine the thickness dependence of the SHG enhancement factor shown in Fig. 2(c), we performed experiments in which the thickness of the MoS_2 layer was reduced by using fs laser ablation while the evolution of the SHG intensity with increasing ablation time was recorded. In Figs. 6(a) and 6(b), we present the nonlinear response spectra measured for the 17-nm-thick MoS_2 layer on the Au/SiO_2 substrate and the 9-nm-thick MoS_2 layer on the SiO_2-SnO_2/Ag/SiO_2 substrate at different irradiation times. The power of the fs laser was chosen to be 80 and 50 mW, respectively. The dependences of the SHG intensity on the irradiation time for the two cases are shown in the insets. A monotonic decrease of the SHG intensity with increasing ablation time is observed for the 17-nm-thick MoS_2 layer. This trend is in good agreement with the prediction based on the numerical simulation. In Fig. 6(b), one can see a reduction of the SHG intensity for ablation times smaller than 120 s. After that, an increase in the SHG intensity followed by a rapid decrease is observed. This behavior is also coincident with that predicted in Fig. 2(c). These results indicate that the thickness dependent SHG has been modified by using different substrates and the relationship between the SHG intensity and the thickness of the MoS_2 layer predicted by using Eq. (1) is reasonable. In addition, it verifies that the SHG in thick MoS layers is dominated by the localization of electric field at the wavelength of the fundamental light rather than the invesion symmetry.

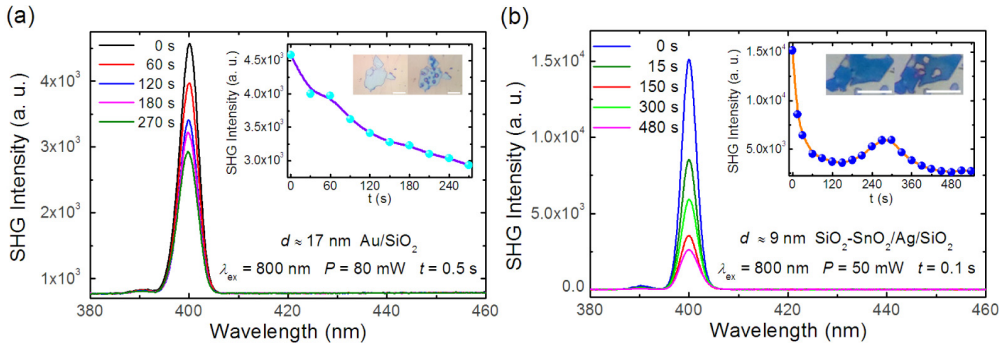

Fig. 6. Nonlinear response spectra measured at different irradiation times for the 17-nm-thick MoS_2 layer on the Au/SiO_2 substrate (a) and the 9-nm-thick MoS_2 layer on the SiO_2-SnO_2/Ag/SiO_2 substrate (b). The dependences of the SHG intensity on the irradiation time and the microscope images before and after the ablation for the two cases are shown in the insets.

4. Conclusion

In summary, we have proposed and demonstrated the use of dielectric-metal hybrid substrates to achieve significantly enhanced SHG in 2D materials by using MoS_2 layers as an example.

#252118 Received 16 Oct 2015; revised 21 Nov 2015; accepted 24 Nov 2015; published 1 Dec 2015

It was found that the strongest SHG was observed in the 17-nm-thick MoS_2 layer on the Au/SiO_2 substrate and the 9-nm-thick MoS_2 layer on the SiO_2-SnO_2/Ag/SiO_2 substrate. The relationship between the linear absorption and the electric field localization has been established and the strongest localization of electric field is expected to occur at a thickness where the largest absorption (or the smallest reflection) is observed. Since the nonlinear optical properties of 2D materials (such as SHG) are quite useful for device applications, our findings are helpful for designing suitable dielectric-metal hybrid substrates to maximize their nonlinear optical responses. For instance, the thickness-dependent SHG in thick MoS_2 samples on the Au/SiO_2 substrate can be exploited to realize optical data storage through the thinning of the thickness by fs laser pulses [39].

Acknowledgments

The authors acknowledge the financial support from the National Natural Science Foundation of China (NSFC) (Grant Nos. 51171066 and 11374109).

#252118 Received 16 Oct 2015; revised 21 Nov 2015; accepted 24 Nov 2015; published 1 Dec 2015